MDPI

Article

Brittle Crack Arrest Temperature Estimation Method Utilizing a Small-Scale Test with a Thick Steel Plate for Shipbuilding

Gyubaek An [1], Jeongung Park [2,*], Daehee Seong [1] and Junseok Seo [3]

1   Department of Naval Architecture and Engineering, Chosun University, Gwangju 61452, Republic of Korea;
    gyubaekan@chosun.ac.kr (G.A.); dae-hee@chosun.kr (D.S.)
2   Department of Civil Engineering, Chosun University, Gwangju 61452, Republic of Korea
3   Energy Steel Application Technology Team, Hyundai Steel, Dangjin 31719, Republic of Korea;
    jss3953@hyundai-steel.com
*   Correspondence: jupark@chosun.ac.kr; Tel.: +82-62-230-7099

Abstract: As the shipbuilding industry has emerged from an extended recession, orders for high-value-added ships, such as LNG and ultra-large container ships, are increasing. For ultra-large container ships, high-strength, thick materials are applied. Because the possibility of brittle fracture increases owing to the application of thick steel plates, the related regulations of the International Association of Classification Societies have been strengthened to prevent brittle fracture. To secure brittle fracture stability, it is necessary to secure crack arrest toughness (K_{ca}) through large ESSO experiments or to secure a crack arrest temperature (CAT) value. Because large-scale experiments require considerable costs and efforts, efforts have increased to examine brittle fracture stability through small-scale tests. In the present study, a technology was developed to predict CAT with small specimens. The CAT prediction formula developed with small specimens makes it possible to accurately predict CAT using data obtained through large-scale experiments.

Keywords: brittle crack arrest; fracture toughness; CAT (crack arrest temperature); thick steel plate; brittle fracture; small-scale test

1. Introduction

With the extended recession in the shipbuilding industry, shipbuilders have focused on ships that require high levels of added value and technology, and efforts have been made to build safer ships. Recently, orders for ships have increased as the shipbuilding industry has emerged from a recession; representative ships include LNG carriers and ultra-large container ships. In particular, the size of container ships has increased, reaching 24,800 TEU (twenty-foot equivalent units) as of 2023. To build such ultra-large container ships, steel plates with a yield strength of 460 MPa and a thickness of 80~100 mm are applied to the superstructure of ships [1–4]. For container ships, high-strength, thick steel plates are applied to the superstructure, owing to their structural characteristics. As the size of structures increases, the demand for thick steel plates increases, along with the range of applied steel plates. Most steel plates utilized in conventional shipbuilding have a thickness of less than 50 mm, resulting in a low awareness of the risk of unstable fracture caused by increased thickness. However, with the increasing size of ships, the thickness of applied steel plates has rapidly increased, along with the increased risk of unstable fracture. Therefore, many studies have been conducted to ensure fracture safety [5–16]. In addition, steel with a high level of brittle crack arrest performance (brittle crack arrest steel (BCA steel)) has recently been developed by domestic and overseas steelmakers to prevent unstable fractures that may occur in thick plates [17]. Along with the development of the new steel, referred to as BCA, the classification societies of each country, including the International Association of Classification Societies (IACS), have enacted guidelines and rules to secure the brittle fracture safety of thick materials [13–20]. The development of

BCA steel, mainly for application in ultra-large container ships, is an issue that has attracted global attention. The IACS also enacted a unified requirement for internationally approved BCA design [21] and defined BCA steel for H/C and U/D in terms of crack arrest toughness (K_{ca}) or crack arrest temperature (CAT). Recently, research has been conducted on unstable fracture safety for high-strength steel plates with a thickness of 80 mm or higher [22,23]. In Japan, active research has been conducted on brittle crack arrest characteristics for thick steel plates [23,24]. In Europe, groups including the Norwegian–German Classification Society have conducted research on brittle crack occurrence characteristics [12]. In Korea, research has been conducted since 2006, when the unstable fracture safety problem of large container ships was internationally raised, and many performance data have been reported [22–24]. Studies on unstable fractures have mostly been conducted to evaluate the brittle crack arrest characteristics of the weld zone of thick steel plates through large fracture tests. According to research conducted in Japan, brittle crack arrest is difficult in the weld zone of steel plates with a thickness of 65 mm or higher [9,10], and the Japan Classification Society revised related regulations to strengthen fracture safety in March 2009 [25]. However, the reported research result considered only the influence of the thickness in evaluating fracture toughness, and the influence of other factors on the welding process was not evaluated. To evaluate the unstable fracture safety of thick materials, K_{ca} or CAT values must be derived through large-scale experiments, such as ESSO experiments. When the rules stipulated by the IACS are satisfied, the materials can be applied to ultra-large container ships. The IACS unified requirement requires a K_{ca} value of 8000 N/mm$^{1.5}$ or higher at −10 °C for a thickness of up to 100 mm to achieve sufficient brittle crack arrest performance [26]. In addition, brittle crack arrest at −10 °C must be observed in a CAT experiment. However, to derive K_{ca} and CAT, fracture toughness must be evaluated with large specimens. Because such evaluation requires considerable cost and time, it is difficult in related industries. Previously, research was conducted to predict CAT through small-scale NRL experiments [5,14,27]. Wisener derived a formula for predicting CAT, considering the influence of the thickness and strength of the applied steel [5,28,29]. Because applying the formula to the latest steel is difficult, a novel prediction formula is required [14].

In this study, an attempt was made to predict CAT through a small-scale test, which is required to stably build ultra-large container ships. To this end, the brittle fracture toughness of the applied steel was evaluated by performing a CAT experiment with large specimens. The nil ductility transition temperature (NDTT) was derived with NRL specimens, which are small, and its correlation with the CAT derived through a large-scale experiment was identified. In addition, a technology to predict the CAT value derived through a large-scale experiment utilizing a small-scale NRL test was developed.

2. Manufacturing of Fracture Toughness Test Specimens

Owing to the structural characteristics of container ships, hatch side coaming, which is the superstructure, is subjected to the largest load, as demonstrated in Figure 1; thus, high-strength, thick steel plates are applied. Because the possibility of brittle fracture increases in thick materials, brittle crack arrest toughness is mainly examined with large-scale experiments. Figure 2 illustrates the steel types applied to large container ships and their maximum thickness by container ship size.

The K_{ca} and CAT values required by the IACS for each thickness are also presented. When the steel thickness is 80 mm or higher, more than 8000 N/mm$^{1.5}$ is required at −10 °C and a CAT value of −10 °C or less. These K_{ca} and CAT values can be obtained through large-scale experiments. Generally, the K_{ca} is calculated with Equation (1). Tables 1 and 2 present the chemical composition and mechanical properties of the specimens utilized in this study. We utilized 460 MPa steel for shipbuilding. It has isometric particles with a grain size of 20 μm through the hot rolling process at approximately 1150 °C. The steel utilized in the experiment meets the basic properties required by the IACS.

$$K_{ca} = \sigma_g \sqrt{\pi C_a} \sqrt{\frac{2B}{\pi C_a} \tan \frac{\pi C_a}{2B}} \tag{1}$$

where σ_g (*P/Bt*) is the applied gross stress (N/mm^2), *P* is the applied load (N), *B* is the specimen width (mm), and *t* is the specimen thickness (mm).
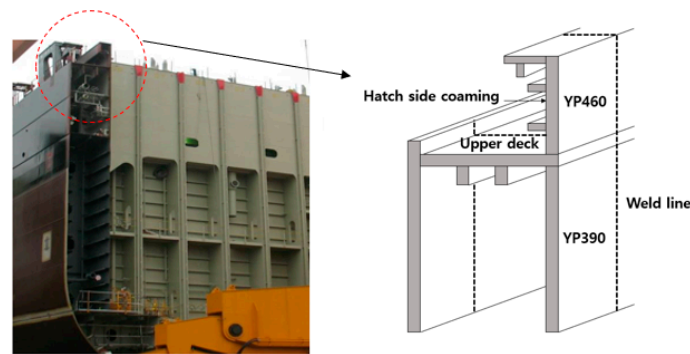

Figure 1. The upper deck structure of a large container ship with a YP460 steel plate.

Figure 2. Steel plate thickness and brittle crack arrestability requirement with an increase in container ship size.

Table 1. Chemical composition of the used steel plates.

Material	Chemical Composition (Mass, %)					
	C	**Si**	**Mn**	**Cu**	**P**	**S**
YP460	$\leq$0.1	$\leq$0.5	$\leq$2.0	$\leq$0.02	$\leq$0.02	$\leq$0.01

Table 2. Mechanical properties of YP460 steel.

Material	Thickness (mm)	Yield Strength (MPa)	Tensile Strength (MPa)	Elongation (%)	Charpy Impact Energy (J, $-40\ ^\circ$C)
YP460	100 mm	497	610	22	270 (transverse)

3. Experimental Procedure

3.1. Large-Scale Brittle Crack Arrest Test Methods

Brittle crack arrest toughness can be secured by evaluating K_{ca} and CAT. Large-scale ESSO tests of brittle crack arrest toughness have recently been widely conducted under

temperature gradient conditions [27,28]. For CAT evaluation, an experiment was performed by facilitating the occurrence of brittle cracks by randomly developing a brittle area with electron beam welding (EBW) and local temperature gradient (LTG). The specimens utilized in the experiment are presented in Figure 3a. The entire thickness was utilized for the specimens, and the width and length were both set to 500 mm. To generate cracks, a fine notch of approximately 0.14 mm was inserted. To prevent the occurrence of shear lip from affecting brittle crack arrest, specimens with side grooves on the surface were applied, as demonstrated in Figure 3b. The characteristics of the conventional CAT experimental method are summarized in Figure 4. In the CAT experiment, a uniform temperature was distributed across the specimen as a target temperature, and the arrest of brittle cracks after propagation for a certain distance was determined. K_{ca} and CAT have the same meaning as the material's mechanical properties. However, K_{ca} is based on the K value, while CAT is based on the temperature. The methods of experimenting by facilitating the occurrence of brittle cracks via the random development of a brittle area with EBW and LTG and the generation of cracks with dummy plates were utilized. The EBW method may affect crack propagation/arrest as defects occur during the EBW process. Therefore, in this study, we performed the CAT experiment with LTG—which requires no preprocessing—to evaluate brittle crack arrest toughness.
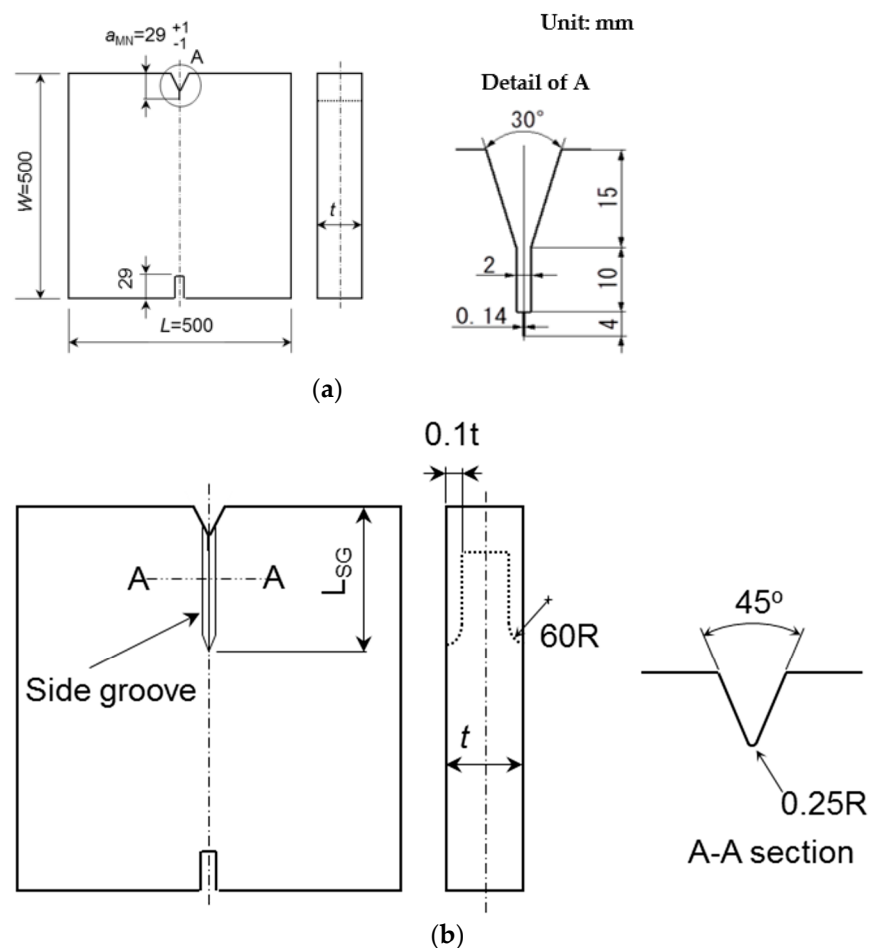

Figure 3. Geometry of the brittle crack arrest test specimen and side groove shape. (**a**) Standard test specimen shape; (**b**) side groove shape.

Items	Impact type		Double tension type
	Electron Beam Weld type	Local Temp. Gradient type	
Models			
Test conditions	▪ Applied stress: 2/3 of SMYS ▪ Test temperature: Isothermal ▪ Crack initiation: Impact load ▪ Pre process: EBW	▪ Applied stress: 2/3 of SMYS ▪ Test temp.: LTG + Iso-thermal ▪ Crack initiation: Impact load ▪ Pre process: No	▪ Applied stress: 2/3 of SMYS ▪ Test temperature: Isothermal ▪ Crack initiation: Tensile load ▪ Pre process: Dummy plate + EBW
Advantages	▪ The exact brittle crack length ▪ Easy temperature management	▪ Not need pre process (like a EB welding)	▪ The exact brittle crack length ▪ Easy temperature management
Disadvantages	▪ Need EB welding ▪ Need temperature gradient at notch tip in high CAT test	▪ Need temperature gradient	▪ Need dummy plate to crack initiation ▪ Need EBW process

Figure 4. Large-scale brittle crack arrest temperature (CAT) test methods.

3.2. Small-Scale Brittle Crack Arrest Test Method

To predict the brittle crack arrest toughness using large specimens in a small-scale test, the NDTT value was derived with NRL specimens, as presented in Figure 5. The experiment was performed following ASTM E208-06 [29], and it was repeated twice in the −65 to −130 °C temperature range. The standard drop-weight test conditions are shown in Table 3 [29]. In this study, a P-2 type specimen was used to evaluate the NDTT. The weight of the hammer utilized in the experiment was 43 kg, and the falling height was 0.95 m. An energy of 400 kgfm was applied. The temperature that resulted in no break in the two repeated experiments was defined as the NDTT.
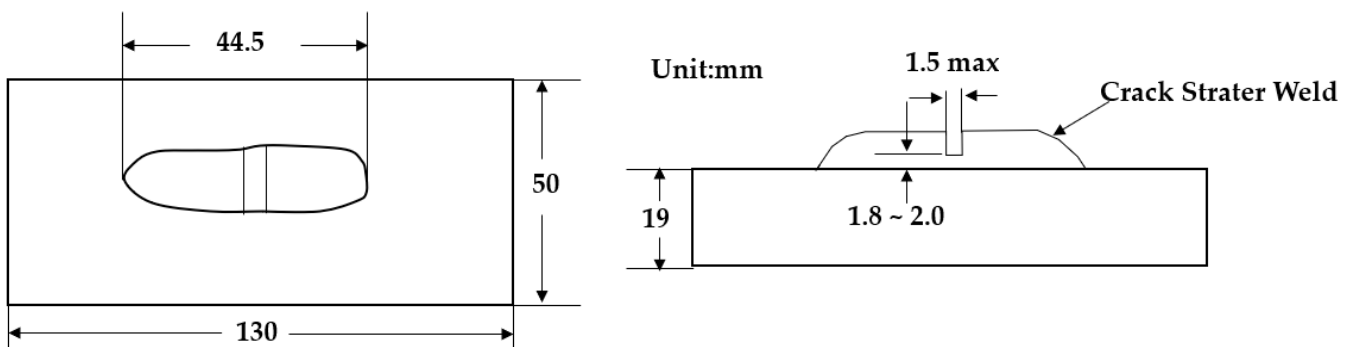

Figure 5. Geometry of the nil-ductility transition temperature test specimen.

Table 3. Standard drop-weight test conditions [29].

Type of Specimen	Specimen Size, mm	Span, mm	Deflection Stop, mm	Yield Strength Level, MPa	Drop-Weight Energy for a Given Yield Strength Level, J
P-1	25.4/89/356	305	7.6	210~340 340~480 480~620 620~760	800 1100 1350 1650
P-2	19/51/127	102	1.5	210~410 410~620 620~830 830~1030	350 400 450 550
P-3	15.9/51/127	102	1.9	210~410 410~620 620~830 830~1030	350 400 450 550

4. Results and Discussion

4.1. Large-Scale Brittle Crack Arrest Test Results

Figure 6 presents the size and geometry of the LTG specimen utilized in the CAT experiment. The size of the specimen was 500 mm (length) × 500 mm (width) × 100 mm (thickness), and a notch of 0.14 mm was inserted to generate brittle cracks. In addition, the influence of the shear lip that may affect brittle crack arrest was removed by inserting a side groove with a depth of approximately 10 mm on both sides of the specimen surface. The CAT experiment of the LTG type was performed by forcibly developing a brittle area by generating a temperature gradient in the 150 mm section in the notch direction. To measure the temperature of the specimen, thermocouples were installed at 50 mm intervals, as demonstrated in Figure 7. The experimental temperature was maintained within ±2 °C of the set temperature. Liquid nitrogen was utilized for cooling. A temperature gradient was generated, and the temperature was managed by attaching a cooling chamber and adjusting the amount of liquid nitrogen. For the section beyond 150 mm, when the target temperature was reached, the temperature was maintained for at least [10 + (0.1 × thickness)] min to secure a uniform temperature distribution in the thickness direction. An impact load was then applied to the front end of the notch to generate brittle cracks. The experimental temperature must be accurately controlled in the 150~350 mm (0.3~0.7 W) range to stop the propagation of brittle cracks. In this section, we evaluate brittle crack arrest performance, and the CAT is determined. In addition, it is necessary to stop the propagation of cracks in the 0.3~0.7 W range to obtain an effective value in the experiment [30]. Meanwhile, the stress applied to the specimen and the initial crack length are important parameters in the CAT evaluation experiment. The CAT value varies depending on the initial crack length and applied load. In ship design, the yield strength and material coefficient of each steel type are considered in setting design stress [6,7]. However, in this study, we determined design stress with two-thirds specific material yield stress [8] to utilize a more conservative approach. For the steel with a yield stress of 460 MPa utilized in this study, 307 MPa was applied as design stress [31].

Generally, CAT is determined via two to three experiments. An experiment is performed under a target temperature −5 °C if the propagation of cracks stops at the target temperature and under a target temperature +5 °C if the propagation of cracks does not stop at the target temperature to set the final range of CAT. Figure 8 presents the samples used in the CAT experiment in this study with their fracture surface and temperature profiles. The CAT experiment of the LTG type was performed with three to four large-scale tests for six different types of charge and the same YP460 grade steel. The experimental results are summarized in Table 4. The six types of specimens achieved similar performance, with

slight differences in tensile strength and yield strength within the standard, as presented in Table 4. CAT was judged to be at $-45\,°C < CAT \leq -30\,°C$. There was a slight difference in CAT depending on the steel charge, but it is judged that the difference is insignificant. The CAT experiment was performed under the same load conditions, and the experimental temperature was adjusted according to the performance of the steel. The steel utilized in this study met the IACS performance requirement.
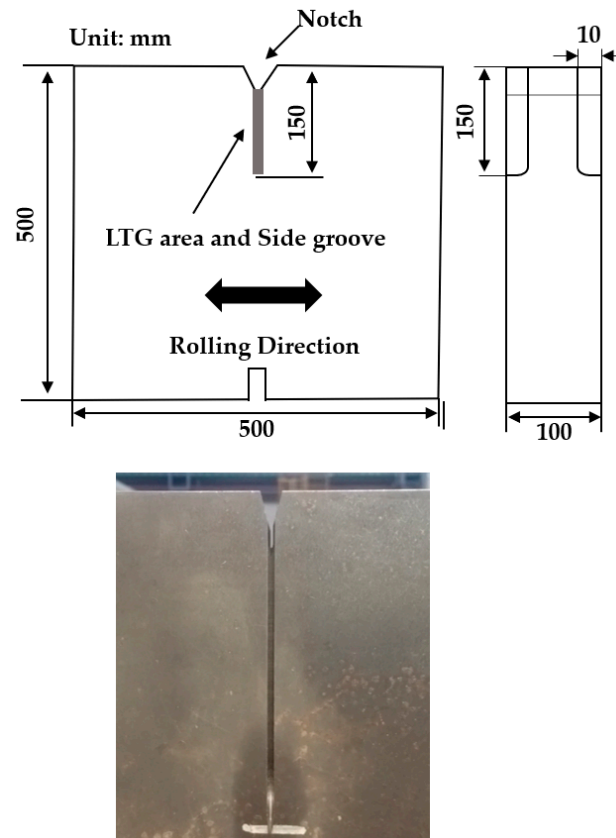

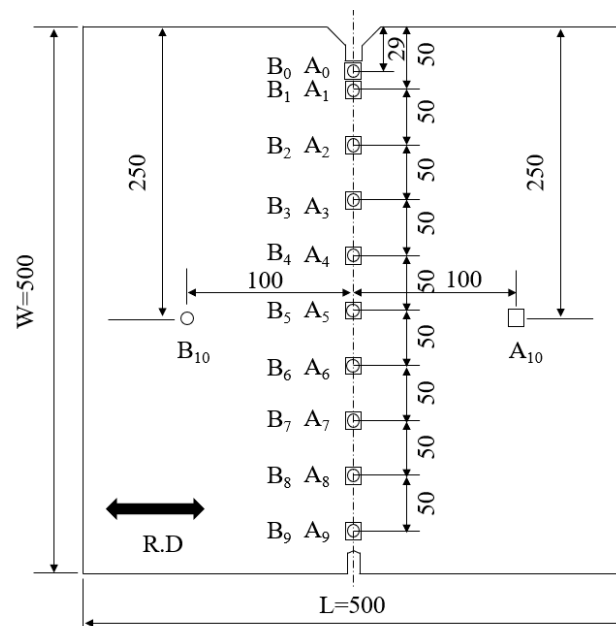**Figure 6.** LTG type brittle crack arrest test specimen.

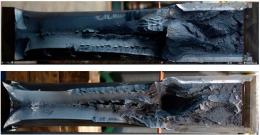**Figure 7.** Temperature gradient profile under LTG embrittlement.

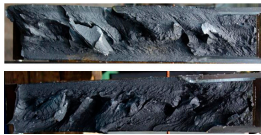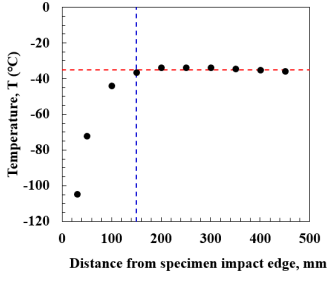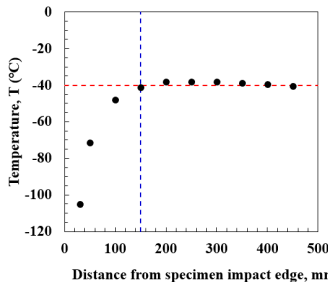| Specimen	LTG #1	LTG #2
Test temp.	−35 °C	−40 °C
Fracture surface		
Temperature gradient profile in LTG zone		
Test conditions	Applied load: 307 MPa	Applied load: 307 MPa
Arrest crack length	168mm	Full propagation

Figure 8. Brittle crack arrest temperature test with LGT type specimens. The blue dashed line show the brittle zone and red dashed line show the target temperature.

Table 4. Summary of crack arrest temperature test results.

Specimen No.	Thickness (mm)	Crack Arrest Temperature Test			
		Applied Stress (MPa)	Test Temp. (°C)	Crack Arrest Length	CAT
1-1			−25	Arrest (170 mm)	
1-2	100	307	−30	Arrest (180 mm)	−35 °C < CAT ≤ −30 °C
1-3			−35	Fracture (500 mm)	
2-1			−25	Arrest (180 mm)	
2-2	100	307	−30	Arrest (185 mm)	−35 °C < CAT ≤ −30 °C
2-3			−35	Fracture (500 mm)	
3-1			−25	Arrest (160 mm)	
3-2	100	307	−30	Arrest (155 mm)	−35 °C < CAT ≤ −30 °C
3-3			−35	Fracture (500 mm)	
4-1			−40	Arrest (161 mm)	
4-2	100	307	−45	Arrest (212 mm)	−45 °C < CAT ≤ −40 °C
4-3			−45	Fracture (500 mm)	
5-1			−35	Arrest (182 mm)	
5-2	100	307	−40	Arrest (207 mm)	−45 °C < CAT ≤ −40 °C
5-3			−40	Arrest (239 mm)	
5-4			−45	Fracture (500 mm)	
6-1			−35	Arrest (229 mm)	
6-2	100	307	−40	Arrest (303 mm)	−45 °C < CAT ≤ −40 °C
6-3			−40	Arrest (303 mm)	
6-4			−45	Fracture (500 mm)	

4.2. Estimate of Brittle Crack Arrest Temperature (CAT) with Small-Scale Specimens

To predict CAT, an NRL experiment was performed at 5 °C intervals in the −65 °C to −130 °C temperature range on the surface and at the center of six types of YP460 steel. The experimental results are presented in Table 5. The NRL experiment was performed following ASTM E208 and repeated twice. There was a difference in the thickness direction because the specimens utilized in this experiment had a thickness of 100 mm. Overall, the surface had a lower NDTT than the center. Figure 9 presents the results of the NRL experiment for which NDTT was −85 °C. All cases where break and no break were mixed in the two repeated experiments were considered to fail, and the temperature that exhibited no break in the two repeated experiments was set as the NDTT. For all specimens, the NDTT value was derived under the same conditions. The CAT test using large-scale specimens and NRL testing using small-scale specimens have something in common in deriving the temperature at which brittle crack arrest occurs. Therefore, we attempted to predict the CAT value derived through a large-scale experiment based on the NRL experimental results. In the CAT experiment, a brittle crack was initiated using impact load and arrest after applying design stress. The NRL experiment was conducted to determine the brittle crack arrest temperature after initiation by impact load. Although there is a difference in the size of the test specimens, both tests were conducted to derive the brittle crack arrest temperature. Therefore, we attempted to derive the CAT value using the small-scale test results.
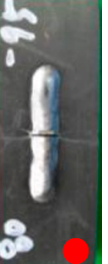
NRL test temperature and specimens (No. 6, Center)							NDTT (℃)
–70 ℃	–75 ℃	–80 ℃	–85 ℃	–90 ℃	–95 ℃	–100 ℃	

Figure 9. NRL test results of specimen No. 6 (Center).

Table 5. Summary of NRL drop-weight test results.

No.	Strength		Test Posi-tions	NRL Test Temperature and Results (°C)														NDTT (°C)
	YP	TS		−65	−70	−75	−80	−85	−90	−95	−100	−105	−110	−115	−120	−125	−130	
1	493	607	S	◑	◑	◑	◑	◑	◑	◑	●	●						−95
				◑	◑	◑	◑	◑	◑	◑	●	●						
			C	◑	●	●												−65
				◑	●	●												
2	496	609	S	◑	◑	◑	◑	◑	◑	◑	●	●						−95
				◑	◑	◑	◑	◑	◑	◑	●	●						
			C	◑	◑	◑	●	●										−75
				◑	◑	◑	●	●										
3	491	603	S	◑	◑	◑	◑	◑	◑	◑	●	●						−100
				◑	◑	◑	◑	◑	◑	◑	●	●						
			C	◑	◑	●	●											−75
				◑	◑	●	●											
4	498	607	S	◑	◑	◑	◑	◑	◑	◑	◑	●	●					−100
				◑	◑	◑	◑	◑	◑	◑	◑	●	●					
			C	◑	◑	◑	●	●										−75
				◑	◑	◑	●	●										
5	504	614	S	◑	◑	◑	◑	◑	◑	◑	◑	◑	◑	◑	◑	◑	●	−125
				◑	◑	◑	◑	◑	◑	◑	◑	◑	◑	◑	◑	◑	●	
			C	◑	◑	◑	◑	●	●									−80
				◑	◑	◑	◑	●	●									
6	495	604	S	◑	◑	◑	◑	◑	◑	◑	◑	◑	◑	●	●			−110
				◑	◑	◑	◑	◑	◑	◑	◑	◑	◑	●	●			
			C	◑	◑	◑	◑	◑	●	●								−85
				◑	◑	◑	◑	◑	●	●								

S: Surface, C: Center ◑: No break; ●: break.

Large-scale tests are required to obtain the CAT value. Because large-scale experiments require considerable cost and time, an attempt was made to derive the CAT value with a simple method. Previously research has been conducted to predict CAT through NRL experimentation [5,14,27], predicting the CAT value according Equation (1). In the equation, [NDTT + 10 °C] was derived for 124 MPa steel with a thickness of 25 mm. Equation (2) [5,14,27] was completed considering various steel types and thicknesses.

$$\text{CAT} = [NDTT + \ 10\,^{\circ}\text{C}] + \left[\frac{ln\sigma}{0.046} - 105\right] + \left[153{\cdot}(B-5)^{\frac{1}{13}} - 190\right] \quad (2)$$

where NDTT is the nil-ductility transition temperature, σ is the yield strength, and B is the specimen thickness.

Because 460 MPa steel with a thickness of 100 mm was applied, it was impossible to accurately predict CAT by applying the conventional prediction formula. Therefore, a novel prediction formula was developed based on the conventional formula. The NRL experimental results were utilized in the same way as in previous research. Because the steel was very thick, the NRL value differed depending on the thickness direction. Therefore, a novel CAT prediction formula was derived based on the values on the surface and at the center, as expressed in Equation (3). The part that considered the material and thickness in

the conventional prediction formula was utilized as it was, and the [NDTT + 10 °C] part was modified to fit the current steel and thickness.

$$CAT_{est.} = \left[\frac{(NDTT_s + NDTT_C)}{2} + 10 \right] + \left[\frac{\ln\sigma}{0.046} - 105 \right] + \left[153 \cdot (B - 5)^{\frac{1}{13}} - 190 \right] \quad (3)$$

Table 6 summarizes the CAT values predicted for six types of YP460 steel. The CAT values derived via the large-scale experimentation are in agreement with those derived through the NRL experiment, i.e., a small-scale test. Figure 10 presents the CAT values predicted via large-scale and small-scale NRL experiments. Overall, it is judged that the CAT value can be predicted with the developed formula despite slight differences.

Table 6. Summary of estimated brittle crack arrest temperature.

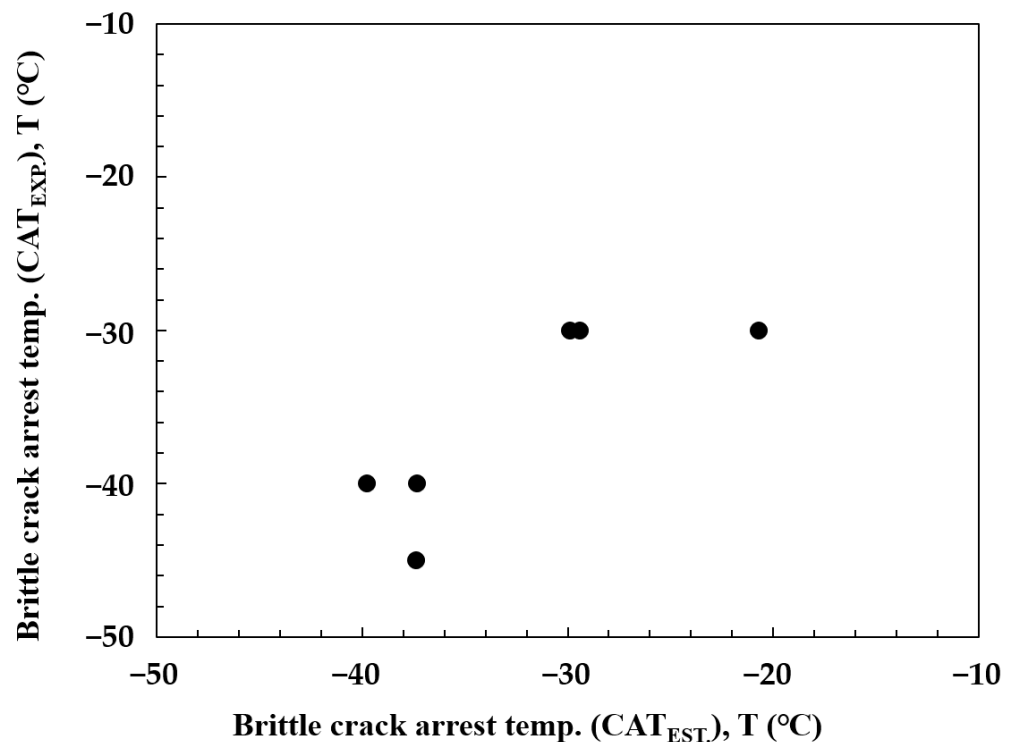| Specimen No.	Thick. (mm)	Applied Stress, σ (MPa)	Surface NDTT$_{(S)}$ (°C)	Center NDTT$_{(C)}$ (°C)	(NDTT$_{(S)}$ + NDTT$_{(C)}$)/2 (°C)	CAT$_{exp.}$ (°C)	CAT$_{est.}$ (°C)
1	100	307	−95	−65	−80	−30	−20.7
2	100	307	−95	−75	−85	−30	−29.4
3	100	307	−100	−75	−87.5	−30	−29.9
4	100	307	−125	−80	−102.5	−40	−37.34
5	100	307	−125	−80	−102.5	−45	−37.4
6	100	307	−110	−85	−97.5	−40	−39.8

Figure 10. Comparison of experimental brittle crack arrest temperature and estimated brittle crack arrest temperature.

Because the CAT value obtained through large-scale experiments can be predicted through the proposed NRL experiment, the proposed method is expected to be useful in deriving the CAT of thick materials.

5. Conclusions

In this study, we attempted to predict the crack arrest temperature (CAT) and the brittle crack arrest toughness of thick, high-strength steel plates for shipbuilding using small specimens such as NRL. In general, CAT was derived utilizing thick specimens with a width of 500 mm or higher, but it was predicted simply using small specimens, owing to the difficulty of the experiment. The results of this study are summarized as follows.

(1) When the brittle crack arrest toughness of YP460MPa steel with a thickness of 100 mm was evaluated, a CAT value of $-10\,^\circ$C or less, as required by the IACS, was obtained, and the requirements were met.

(2) When the NRL small-scale test was conducted on the surface and at the center, the surface's toughness was higher than that at the center because the material did not have homogeneous properties in the thickness direction, owing to the nature of the thick material. The temperature difference was found to be approximately $30\,^\circ$C.

(3) To apply the NDTT obtained from small NRL specimens to thick materials, a formula for predicting CAT was developed by deriving NDTT on the surface and at the center in the thickness direction. This prediction formula makes it possible to predict the CAT of thick materials, such as materials with a thickness of 100 mm, through NRL experiments.

Author Contributions: Conceptualization, G.A.; Software, J.S.; Validation, D.S.; Formal analysis, G.A. and J.P.; Investigation, D.S.; Resources, J.S.; Data curation, J.P.; Writing—original draft, G.A. All authors have read and agreed to the published version of the manuscript.

Data Availability Statement: The data presented in this study are available in article.

Conflicts of Interest: Author Junseok Seo was employed by the company Hyundai Steel. The remaining authors declare that the research was conducted in the absence of any commercial or financial relationships that could be construed as a potential conflict of interest.

Abbreviations

LNG	Liquified natural gas
TEU	Twenty-foot equivalent units
IACS	International Association of Classification Societies
BCA	Brittle crack arrest steel
H/C	Hatch side coaming
U/D	Upper deck
CAT	Crack arrest temperature
$CAT_{est.}$	Estimated CAT
NDTT	Nil-ductility transition temperature
$NDTT_s$	Surface NDTT
$NDTT_c$	Center NDTT
K_{ca}	Brittle crack arrest toughness
EBW	Electron beam welding
LTG	Local temperature gradient
ASTM	American Society for Testing Materials

References

1. Inoue, T.; Ishikawa, T.; Imai, S.; Koseki, S.T.; Hirota, K.; Tada, M. Long crack arrestability of heavy-thick shipbuilding steels. In Proceedings of the 16th International Offshore and Polar Engineering Conference, San Francisco, CA, USA, 28 May–2 June 2006; Volume 4, pp. 132–136.
2. Kawabata, T.; Inoue, T.; Tagawa, T.; Fukui, T.; Takashima, Y.; Shibanuma, K.; Aihara, S. Historical review of research on brittle crack propagation arresting technology for large welded steel structures developed in Japan with the application of Kca parameters. *Mar. Struct.* **2020**, *71*, 80–87. [CrossRef]
3. Handa, T.; Matsumoto, T.; Yajima, H.; Aihara, S.; Yoshinari, H.; Hirota, K. Effect of structural discontinuities of welded joints on brittle crack propagation behavior—Brittle crack arrest design for large container carrier ships. In Proceedings of the 20th International Offshore and Polar Engineering Conference, Beijing, China, 20–25 June 2010; Volume 4, pp. 88–94.
4. Inoue, T.; Yamaguchi, Y.; Yajima, H.; Aihara, S.; Yoshinari, H.; Hirota, K. Required brittle crack arrest toughness Kca value with actual scale model tests-brittle crack arrest design for large container carrier ships. In Proceedings of the 20th International Offshore and Polar Engineering Conference, Beijing, China, 20–25 June 2010; Volume 4, pp. 95–101.
5. Wiesner, C.S.; Hayes, B.; Smith, S.D.; Willoughby, A. Investigations into the Mechanics of Crack Arrest in Large Plates of 1.5%Ni TMCP Steel. *Fatigue Fract. Eng. Mater. Struct.* **1994**, *17*, 221–233. [CrossRef]
6. An, G.B.; Bae, H.Y.; Park, J.U. A Study of Brittle Crack Arrestability Test Method. *J. Weld. Join.* **2020**, *38*, 535–542. [CrossRef]
7. Jang, Y.C.; Lee, Y.S.; An, G.B.; Park, J.S.; Lee, J.B.; Kim, S.I. Temperature dependent fracture model and its application to ultra heavy thick steel plate used for shipbuilding. *Int. J. Mod. Phys. B* **2008**, *22*, 5483–5488. [CrossRef]
8. Shibanuma, K.; Tu, S.; Suzuki, S.; Yu, Z.; Kato, R.; Hatamoto, A. Ductile crack propagation path depending on material properties: Experimental results and discussions based on numerical simulations. *Mater. Des.* **2022**, *223*, 111158. [CrossRef]
9. Machida, S.; Yoshinari, H.; Yasuda, M.; Aihara, S.; Mabuchi, H. Fracture mechanical modeling of brittle fracture propagation and arrest of steel (1)—A fundamental model. *J. Jpn. Soc. Nav. Archit. Ocean Eng.* **1995**, *177*, 243–257. [CrossRef]
10. Aihara, S.; Machida, S.; Yoshinari, H.; Mabuchi, H. Fracture mechanical modeling of brittle fracture propagation and arrest of steel (2)—Application to temperature-gradient type test. *J. Jpn. Soc. Nav. Archit. Ocean Eng.* **1996**, *178*, 545–554.
11. Aihara, S.; Machida, S.; Yoshinari, H.; Tsuchida, Y. Fracture mechanical modeling of brittle fracture propagation and arrest of steel (3)—Application to duplex type test. *J. Jpn. Soc. Nav. Archit. Ocean Eng.* **1996**, *179*, 389–398. [CrossRef]
12. Bertolo, V.; Jiang, Q.; Terol, S.M.; Riemslag, T.; Walters., C.L.; Sietsma, J.; Popovich, V. Cleavage fracture micromechanisms in simulated heat affected zones of S690 high strength steels. *Mate. Sci. Eng. A* **2023**, *868*, 144762. [CrossRef]
13. Chen, L.; Hu, Y.; Yang, K.; Yan, X.; Yu, X.; Yu, J.; Chen, S. Fracture process characteristic study during fracture propagation of a CO_2 transport network distribution pipeline. *Energy* **2023**, *283*, 129060. [CrossRef]
14. Smedley, G.P. Prediction and specification of crack arrest properties of steel pipe. *Int. J. Press. Vessel. Pip.* **1989**, *40*, 279–302. [CrossRef]
15. Sumi, Y. Computational crack path prediction for brittle fracture in welding residual stress fields. *Inter. J. Fract.* **1990**, *44*, 189–207. [CrossRef]
16. Priest, A.H. An energy balance in crack propagation an arrest. *Eng. Fract. Mech.* **1998**, *61*, 231–251. [CrossRef]
17. Yamaguchi, Y.; Yajima, H.; Aihara, S.; Yoshinari, H.; Hirota, K.; Toyoda, M. Development of guidelines on brittle crack arrest design brittle crack arrest design for large container carrier ships. In Proceedings of the 20th International Offshore and Polar Engineering Conference, Beijing, China, 20–25 June 2010; pp. 71–79.
18. Nippon Kaiji Kyokai. *Guidelines of the Application of YP47 Steel for Hull Structures of Large Container Carriers*; Nippon Kaiji Kyokai: Tokyo, Japan, 2008.
19. Gremanischer Lloyd. *Supplementary Rules for Application of Steel with Yield Strength of 460N/mm2*; Gremanischer Lloyd: Hamburg, Germany, 2008.
20. American Bureau of Shipping. *Regulations of the Classification and Registry of Ships*; American Bureau of Shipping: Houston, TX, USA, 2008.
21. Unified Rule S33. *Requirements for Use of Extremely Thick Steel Plates in Container Ships Unified Rule S33*; International Association of Classification Societies: London, UK, 2013.
22. Handa, T.; Kubo, T.; Kawabata, F.; Nishimura, K.; Suzuki, S.; Shiomi, H.; Miyata, T. Effect of Kca value on behavior of brittle crack arrest in Tee joint structure of thick plate. *Bull. Jpn. Soc. Nav. Archit. Ocean Eng.* **2007**, *4*, 459–460.
23. Taylor, J.; Mehmanparast, A.; Kulka, R.; Moore, P.; Xu, L.; Farrahi, G.H. Experimental study of the relationship between fracture initiation toughness and brittle crack arrest toughness predicted from small-scale testing. *Theo. Appli. Frac. Mech.* **2020**, *110*, 102799. [CrossRef]
24. Handa, T.; Suzuki, S.; Toyoda, M.; Yokura, T.; Kiji, N.; Nakanishi, Y. Behavior of long brittle crack arrest in Tee joint structure of thick plate. *Bull. Jpn. Soc. Nav. Archit. Ocean Eng.* **2007**, *4*, 461–462.
25. Nippon Kaiji Kyokai. *W31 YP47 Steels and Brittle Crack Arrest Steels*; Nippon Kaiji Kyokai: Tokyo, Japan, 2023.
26. *WES 2815*; Test Method for Brittle Crack Arrest Toughness. The Japan Welding Engineering Society: Tokyo, Japan, 2014.
27. Wiesner, C.S.; Hayes, B. *A Review of Crack Arrest Tests, Models and Applications*; TWI report; TWI Ltd.: Cambridge, UK, 1995.
28. An, G.B.; Bae, H.Y.; Park, J.U. Development of Crack Arrest Temperature Test Method by Using a Local Temperature Gradient. *J. Test. Eval.* **2020**, *48*, 4241–4248. [CrossRef]

29. *ASTM E208-06*; Standard Test Method for Conducting Drop-Weight Test to Determine Nil-Ductility Transition Temperature of Ferritic Steels. American Society for Testing and Materials: West Conshohocken, PA, USA, 2012.

30. Oie, N.; Kawabata, T.; Kishiki, S.; Nakagomi, T. Specimen size effect on the brittle fracture properties of steel for buildings subjected to large earthquakes. *Procedia Struct. Integr.* **2021**, *33*, 586–597. [CrossRef]

31. Taylor, J.; Mehmanparast, A.; Kulka, R.; Moore, P.; Hossein, G.F.; Xu, L. Compact crack arrest testing and analysis of EH47 shipbuilding steel. *Theo. Appl. Frac. Mech.* **2021**, *114*, 103004. [CrossRef]